

SIS18 closed orbit correction using a local bump method

A. Parfenova, G. Franchetti, B. Franczak, M. Kirk, C. Omet

GSI, 64291 Darmstadt, Germany

November 10, 2006

Abstract

A three-bump local orbit distortion method was applied to the SIS18 closed orbit (CO) correction. We report on several measurement campaigns on closed orbit measurement and correction carried out in February-May 2006. The details of closed orbit measurements and results of the correction are presented.

1 The SIS18 equipment for closed orbit measurement and correction

The CO correction is important for machine operation. The better the CO is corrected, the less beam loss occurs during machine operation due to increase of the machine's acceptance. CO errors are also relevant for feed down effects of multipoles, which may excite beam loss [1].

The SIS18 has 12 periods and a nominal working point at injection energy with tunes (4.29;3.29). There are 24 analog beam position monitors (BPMs): 12 in the horizontal and 12 in the vertical plane [2]. The BPMs are placed in pairs (horizontal and vertical) in every period before the dipoles. The BPMs have separate pickup plates and allow independent CO measurements. In SIS18 6 horizontal and 12 vertical steerers are available for CO control and correction. The vertical steerers are located in every period after the first quadrupole. The horizontal steerers are implemented as correction coils in the dipole magnets and are located in the first dipole of the periods 1, 3, 5, 9 and 12. The horizontal steerer in period 6 is in the second dipole. At extraction energy two more steerers in the 10th and 11th period are available in the first dipole. In Fig. 1a the BPM- and steerer-locations for one SIS18 cell are shown.

2 Description of the experiment campaign

The measurement campaigns during February-May 2006 were performed in order to measure the Orbit Response Matrix (ORM) [3] of SIS18. This matrix will be used to retrieve the SIS18 linear optics, which will appear in a future GSI internal note. Once the linear optics is known, the improvement of SIS18 performance can be studied through linear optics codes such as MAD or MIRKO. However, while measuring the ORM, as an intermediate step, we corrected the CO by a local bump method [4]. All measurements were taken with different ions, energies and tunes. The multiturn injection was set to fill SIS18 acceptance. The order of intensity and injection energy were kept about the same. Detailed information about the measurements is presented in Table 1. The low intensity level for ORM measurements was required in order to exclude the influence of space charge on the beam position.

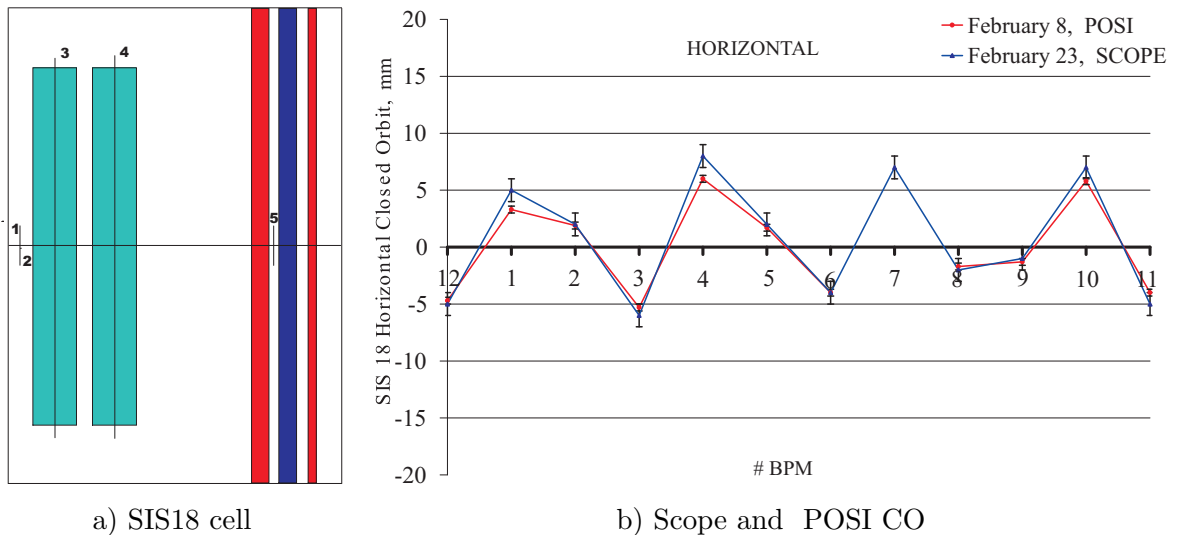


Figure 1: a) One SIS18 cell: 1,2 - horizontal and vertical BPMs; 3,4 - horizontal steerers located in first/second dipoles; 5 - vertical steerer; b) Relative SIS18 CO measured by scope and POSI [5].

3 Test on closed orbit measurements

To start the measurement, several cross checks of CO diagnostics were done. To measure the beam averaged position, two data acquisition systems are available: 1) directly by

Table 1: CO and ORM measurement campaigns in February-May 2006.

Measurement campaign	Ion, extraction energy, MeV/u	Injection energy, MeV/u	Operating tunes	Order of intensity
February 8,	$^{12}C^{6+}$, 200.00	11.528	(3.29;4.29)	10^9
February 23-28, March 1,	$^{107}Ag^{43+}$, 300.00	11.165	(3.29;4.29)	10^9
March 15,	$^{40}Ar^{18+}$, 350.00	11.290	(3.29;4.29)	10^9
April 5-8,	$^{86}Kr^{34+}$, 11.24	11.241	(3.29;4.29)	10^9
April 18-20,	$^{40}Ar^{18+}$, 200.00	11.380	(4.17;3.35) (3.29;4.29)	10^9
May 1-2,	$^{30}Si^{14+}$, 11.38	100.000	(4.17;3.35)	10^9

oscilloscope and 2) with the POSI program [5]. The use of the scope requires development software for data acquisition. Using POSI is faster, because the acquisition of all BPMs is automated and summarized into output files, which can be used for offline data analysis. Consequently we used POSI for the CO studies. By setting the measurement time in POSI one can properly set the storage time (turns) of the CO data. From the average over the stored data the averaged beam position is retrieved. In POSI there is the possibility to start measuring beam position at different initial times, by hardwiring the event in the electronic room. The default setting for the POSI start is at the "beginning of acceleration ramp", but it can be changed to any arbitrary event (to the "beginning of injection" or to the "beginning of extraction"). During the experimental campaign an upgrade of the POSI software was implemented in order to extract more realistic CO data [6]. In all measurements POSI was run in "Narrow band" mode [5]. Oscilloscope CO measurements also provided a complementary good crosscheck of the POSI results.

3.1 Test 1: Comparison of scope and POSI measurement

As a first test we measured the difference between CO when the correction steerers are present and when they are switched OFF. The existing corrector setting was taken by B. Franczak in 1989. In Fig. 1b we show the results: the red and blue curves represent POSI and oscilloscope measurements respectively. Note BPM #7 was absent in this POSI measurement. The agreement between the scope and POSI curves is within the error-bars.

3.2 Test 2: Comparison of MAD, MIRKO predictions with measurements

Simulations with MAD and MIRKO of the CO with correction ON and OFF were done in order to compare the relative CO shifts with the POSI measurements (see Figs. 2 and 3). In the horizontal plane MAD and MIRKO differ a little due to different dipole modelling. The red curve on both pictures is the POSI measurement made on February 8. The vertical BPMs #7 and #8 were also absent in this measurement. We find that the relative experimental horizontal and vertical CO curves do not fully overlap the theoretical ones. To fit them completely the ORM analysis is required.

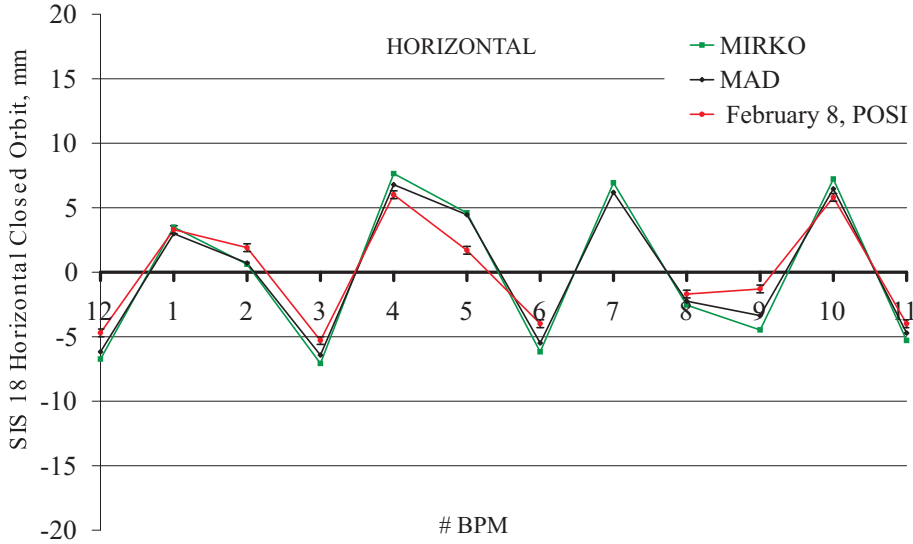


Figure 2: Relative (the difference between steerers ON and OFF) horizontal CO, black curve - MAD calculation, green curve - MIRKO calculation, red curve - February 8th CO measurement.

3.3 Test 3: Reproducibility of closed orbit measurements with POSI

The reproducibility of the relative CO measurements for a fixed tune is important. In order to control it we put on the same plot, see Figs. 4 and 5, the relative POSI CO measurements of several experimental campaigns. The tune was set to (4.29, 3.29) and all the CO curves of Figs. 4 and 5 were taken at injection energy. Unfortunately, from experiment to experiment the number of functioning BPMs was not constant. Nevertheless, the reproducibility of the CO for different measurements can be clearly seen. This test was

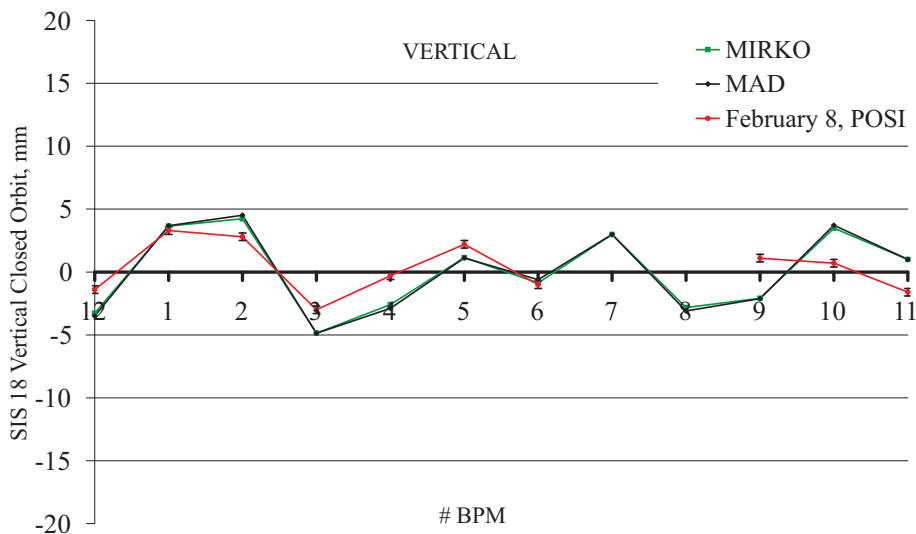


Figure 3: Relative (the difference between steerers ON and OFF) vertical CO, black curve - MAD calculation, green curve - MIRKO calculation, red curve - February 8th CO measurement.

performed before every measurement campaign to be sure that the POSI set up is correct. The CO measurements in Figs. 4 and 5 were performed on different days with different conditions (see Table 1). The reproducibility therefore is not better than ± 1.75 (or 2) mm for the horizontal CO and ± 1 mm for the vertical CO.

4 Three-bump local orbit distortion method and its application in SIS18 for correcting the closed orbit

The CO can be locally corrected at specified locations using steering dipoles by means of the three-bump method, where three steering dipoles are used to adjust local-orbit distortion. Lets take any three steering magnets of the SIS18 ring, see Fig. 6, and let θ_1 , θ_2 and θ_3 be the three bump angles of these steering magnets. The condition of the local bump leaves unchanged the orbit at steerers 1 and 3 so that the CO outside of the steerer region 1-3 remains unchanged. This requirement sets a constraint between the angles θ_1 ,

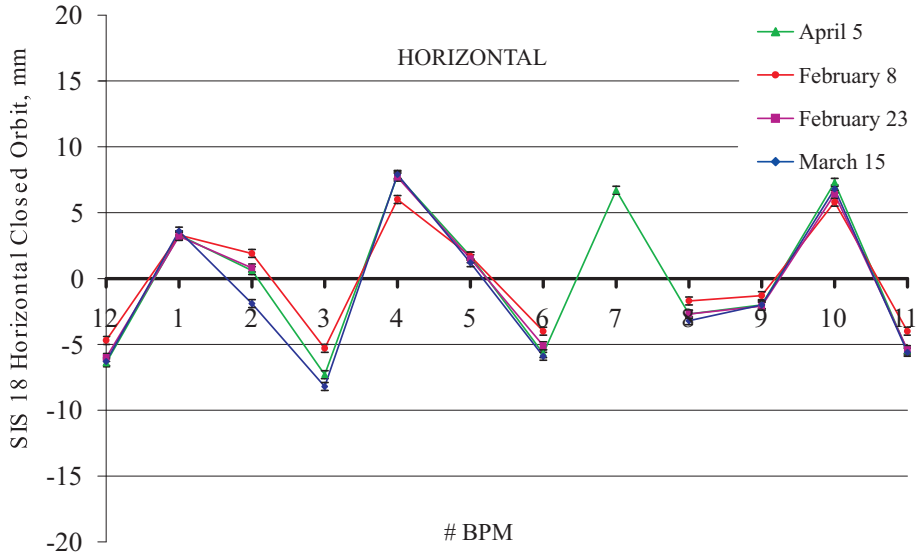


Figure 4: Reproducibility of the horizontal CO in POSI measurements.

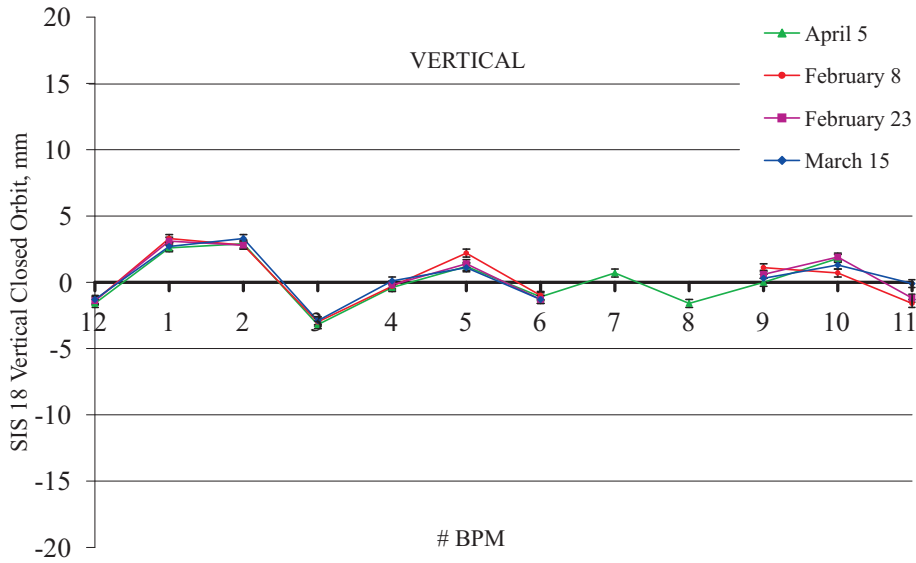


Figure 5: Reproducibility of the vertical CO in POSI measurements.

θ_2 and θ_3 according to [4]

$$\begin{aligned}
 \theta_1 &= \text{free parameter} \\
 \theta_2 &= -\theta_1 \sqrt{\frac{\beta_1 \sin \psi_{31}}{\beta_2 \sin \psi_{32}}} \\
 \theta_3 &= \theta_1 \sqrt{\frac{\beta_1 \sin \psi_{21}}{\beta_3 \sin \psi_{32}}}
 \end{aligned} \tag{1}$$

where β_i is the β -function at the i th steering magnet, $\psi_{ij} = \psi_i - \psi_j$ is the phase advance from the i th to the j th steering dipole. Note that in Eq. 1 the steering angle θ_1 is a free parameter which allows a 'control' on the CO deformation between steerer 1-3.

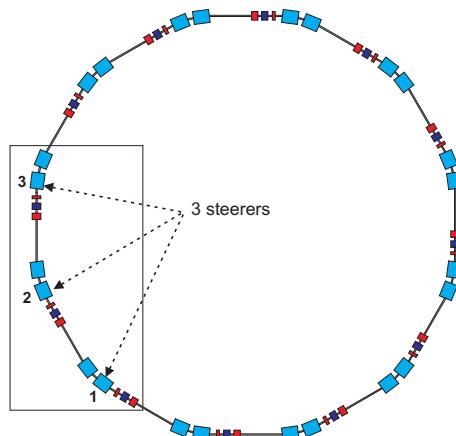


Figure 6: The SIS18 ring with three periods marked. Three steerers are indicated with arrows.

If steering dipoles are located in the same positions in every period (symmetry), the dependence of the β -function in Eq. 1 is removed, as $\beta_1 = \beta_2 = \beta_3$. For this reason the bump angles in Eq. 1 are only dependent on the phase advance between the steering dipoles, which could be written as

$$\psi_{ij} = (j - i)\Delta\psi \quad (2)$$

where $\Delta\psi = \frac{2\pi Q}{N}$, $N = 12$ - number of periods, and Q is the horizontal/vertical tune. For three neighbouring vertical steerers symmetrically located in each of the 12 periods, Eq. 1 becomes

$$\begin{aligned} \theta_1 &= \text{free parameter} \\ \theta_2 &= -\theta_1 \frac{\sin 2\Delta\psi}{\sin \Delta\psi} \\ \theta_3 &= \theta_1 \end{aligned} \quad (3)$$

For applying Eq. 3 no optical functions are needed; only the phase advance between steering dipoles, calculated according to Eq. 2.

When applying the three-bump method in SIS18 experiments, the effect of the CO local bump was simulated in MAD by using the above described formulas for the horizontal

Table 2: The SIS18 steering angles for the vertical local orbit distortion in Fig.7.

steering angles (θ -sets)	curves 1 and 4	curves 2 and 5	curves 3 and 6
θ_1	0.10	0.50	1.0
θ_2	0.03	0.15	0.3
θ_3	0.10	0.50	1.0
θ_7	-0.10	-0.50	-1.0
θ_8	-0.03	-0.15	-0.3
θ_9	-0.10	-0.50	-1.0

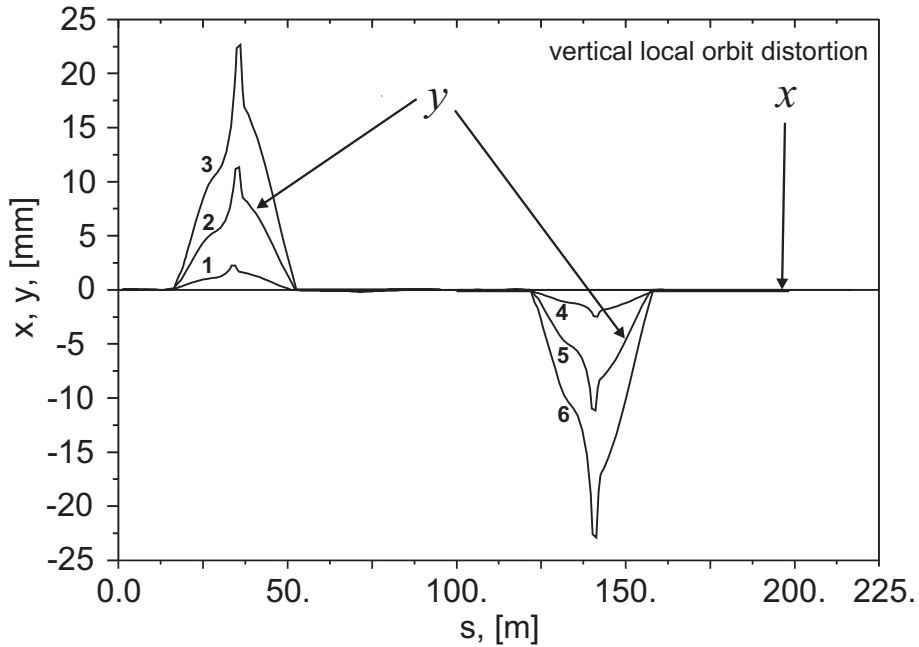


Figure 7: Simulation for SIS18 lattice of two sets of vertical local CO distortions using three steering dipoles in the 1st, 2nd, 3rd period, and in the 7th, 8th, 9th period.

and vertical plane. In Fig. 7 is shown the effect of the vertical local orbit distortions in the presence of two sets of steerers. The first set is formed by using the steering dipoles in the 1st, 2nd and 3rd periods. The second set is formed by the steering dipoles in 7th, 8th and 9th periods. These two sets differ in the direction of bumping by the sign of θ_1 . The settings for θ_1 , θ_2 and θ_3 calculated by Eq. 3 are summarized in Table 2. The angles

θ are in mrad. From Fig. 7 and Table 2 one can see that curves 1, 2 and 3 differ from each other by the strength of the bump angles, similarly for curves 4, 5 and 6.

The three-bump method can be applied to a distorted closed orbit by bumping the CO with the proper angle calculated by Eq. 1, in the opposite direction of distortion, so as to improve the CO distortion. Following this strategy in each plane the CO can be consequently corrected at all positions by altering all steerer in groups of three. For the vertical plane where 12 steerers are available a scheme which uses all steerers permutations is applied. It is not necessary that all three steerers are located in neighbouring periods. In the horizontal plane (at injection energy) we have only six steerers available and the steerers' combinations could then be: (1 3 5) (3 5 6) (5 6 9) (6 9 12) (9 12 1) (12 1 3) or (3 5 9). The example of applying Eq. 1 for the last combination (3 5 9) of horizontal steerers is presented in Fig. 8 with steerer angles reported in Table 3. Due to the symmetrical locations of the 3rd, 5th and 9th steerers in every first dipole Eq. 1 reads

$$\begin{aligned}
\theta_3 &= \text{free parameter} \\
\theta_5 &= -\theta_3 \frac{\sin 6\Delta\psi}{\sin 4\Delta\psi} \\
\theta_9 &= \theta_3 \frac{\sin 2\Delta\psi}{\sin 4\Delta\psi}
\end{aligned} \tag{4}$$

Note that steerer #6 is located in the second dipole (not symmetric to the others). Calculations of bump angles using this steerer should be done by Eq. 1 including the β -functions (β -function for SIS18 is different for injection and extraction energy).

Table 3: The SIS18 steering angles for the horizontal local orbit distortion in Fig.8.

steering angles (θ -sets)	curve 1 (blue)	curve 2 (red)	curve 3 (green)
θ_3	0.100	0.500	1.00
θ_5	-0.183	-0.915	-1.83
θ_9	-0.227	-1.135	-2.27

For implementing the local CO distortion correction the steerers should be well calibrated. If the ratio between θ_1 , θ_2 and θ_3 calculated according to Eq. 1 is broken because of bad steerers' calibration, then the creation of a local CO distortion is impossible. In this case the CO will be globally distorted along the machine.

In Figs. 9 and 10 an example of measured vertical local SIS18 CO distortions is presented. Four values of θ_1 namely -1.0, -0.5, 0.5, 1.0 mrad were used for finding the corresponding

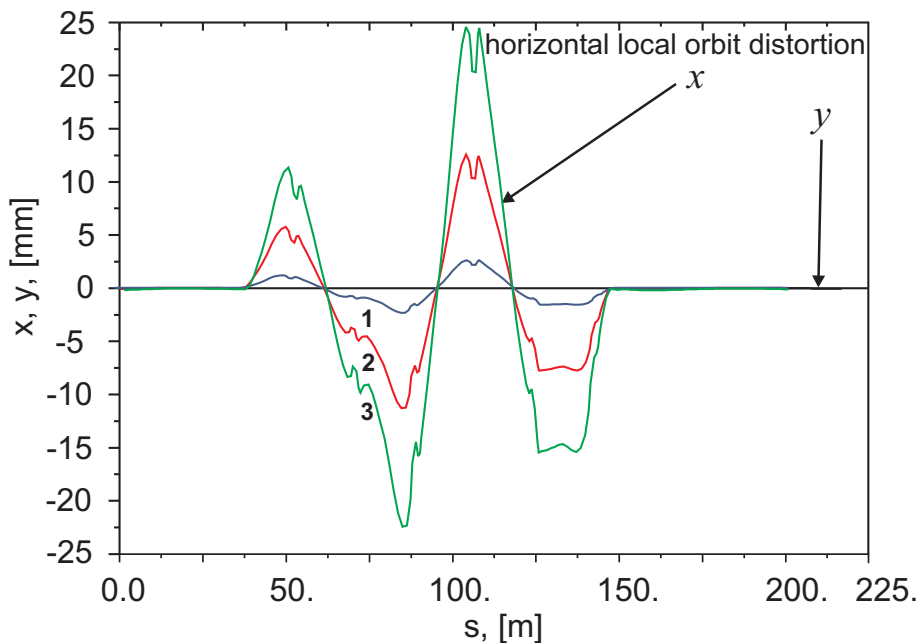


Figure 8: Simulation of the SIS18 lattice with three horizontal local CO distortions using three steering dipoles in the 3rd, 5th, 9th period: curve 1 (blue), curve 2 (red), curve 3 (green).

four θ_2 and four θ_3 . Every set of θ_1 , θ_2 and θ_3 gives a local distortion to the CO, see Fig. 9. The BPM #8 didn't function during the measurements and was excluded. The BPM #4 from time to time gave measurement errors (see Fig. 9 magenta curve and Fig. 10 black curve). In Fig. 9 is shown that the local orbit distortion is reproduced better than in Fig. 10. In Fig. 9 the distortion from the 1st, 2nd, and 3rd steerers is localized in between the 1st and 3rd steerers (see BPMs #1 and #2, which are located in between the 1st and 3rd steerers). In Fig. 10 is shown an "imperfect" local orbit distortion (CO is distorted globally a little), that means that one of the three steerers (9, 10, 11) has a gain factor a little different from 1.

5 Closed orbit correction

We list here in Figs. 11, 12, 13, 14 horizontal and vertical CO before and after correction for injection and extraction energy. The figures represent the CO at high intensity working point: the horizontal and vertical tunes are (4.17, 3.35). In the Tables 4 and 5 the

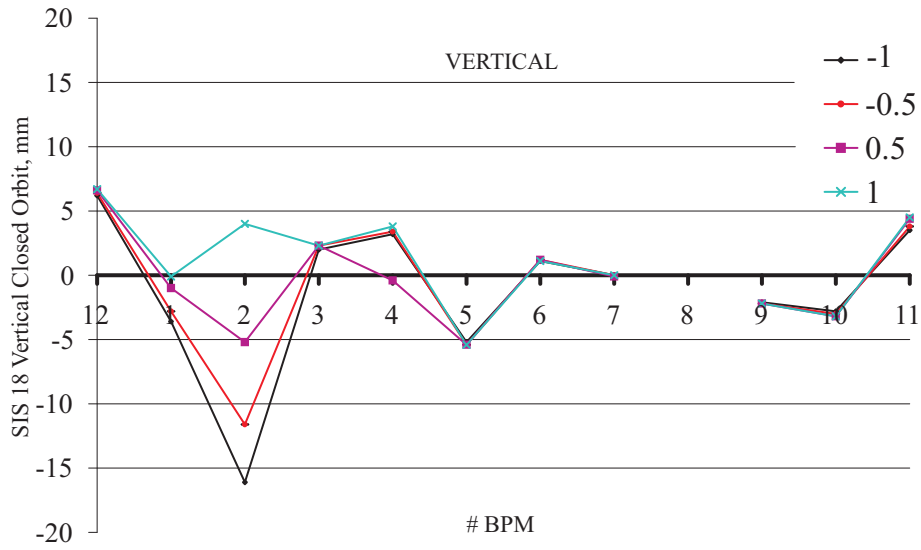


Figure 9: Local vertical CO distortion of different strength created by the 1st, 2nd, 3rd vertical steerers in the SIS18, measured by POSI: black curve - $\theta_1 = -1.0$ mrad; red curve - $\theta_1 = -0.5$ mrad; magenta curve - $\theta_1 = 0.5$ mrad; blue curve - $\theta_1 = 1.0$ mrad.

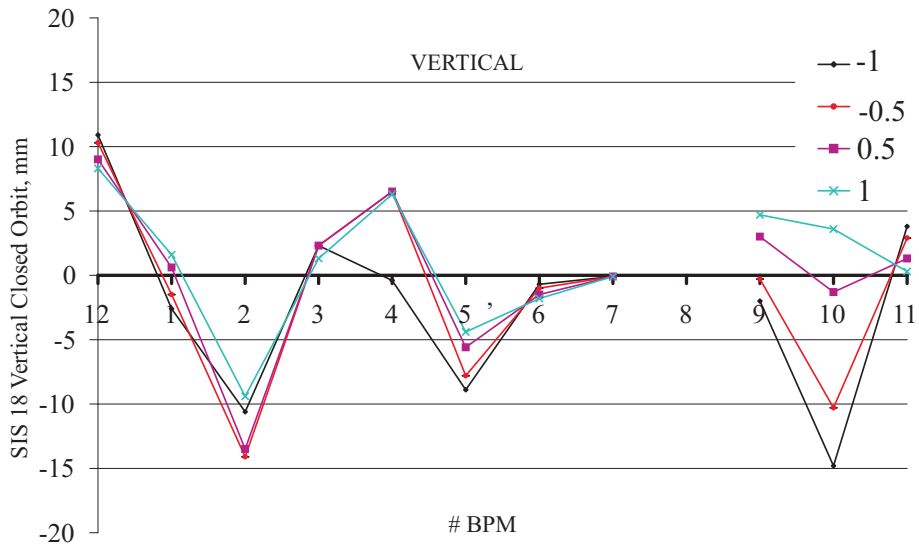


Figure 10: Local vertical SIS18 CO distortion of different strength created by the 9th, 10th, 11th vertical steerers in the SIS18, measured by POSI: black curve - $\theta_1 = -1.0$ mrad; red curve - $\theta_1 = -0.5$ mrad; magenta curve - $\theta_1 = 0.5$ mrad; blue curve - $\theta_1 = 1.0$ mrad.

correction steerer angles are given in mrad. These correction values are saved in the accelerator's control software and currently used.

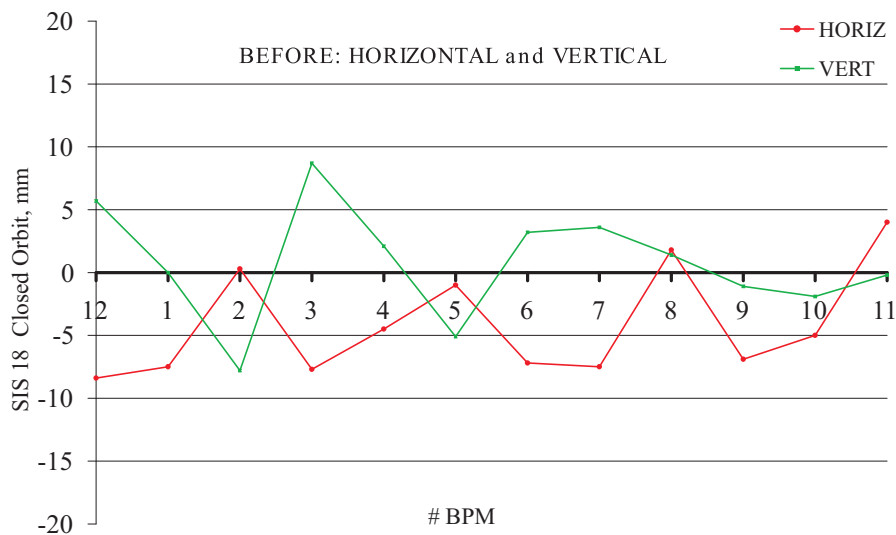


Figure 11: The horizontal and vertical CO at injection energy before correction.

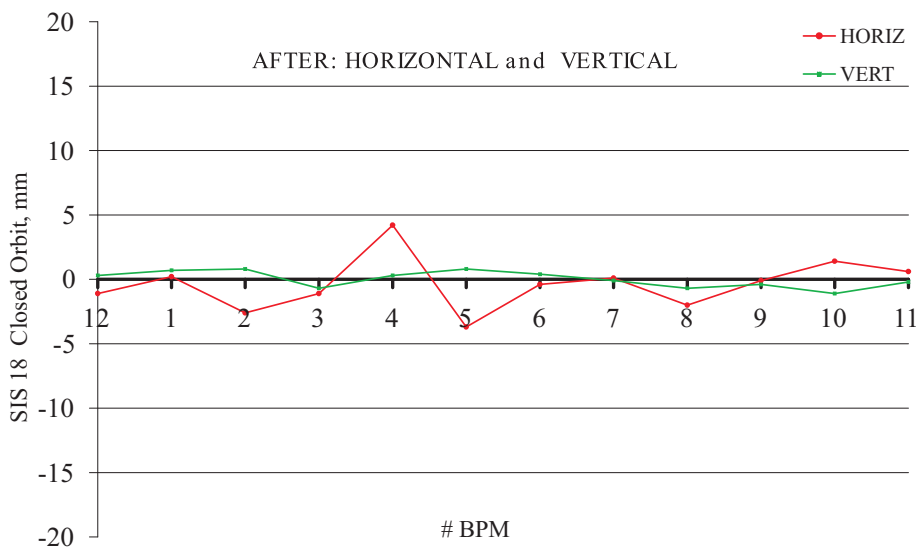


Figure 12: The horizontal and vertical CO at injection energy after correction.

Using the 12 vertical steerers, the vertical CO was brought to a straight line with near to zero mm displacement. As already mentioned, the BPM calibration gains should be

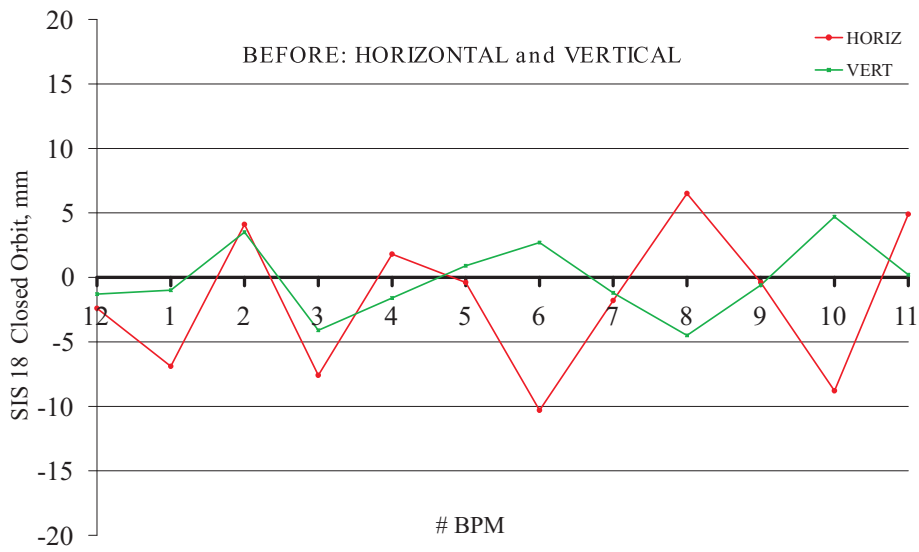


Figure 13: The horizontal and vertical CO at extraction energy before correction.

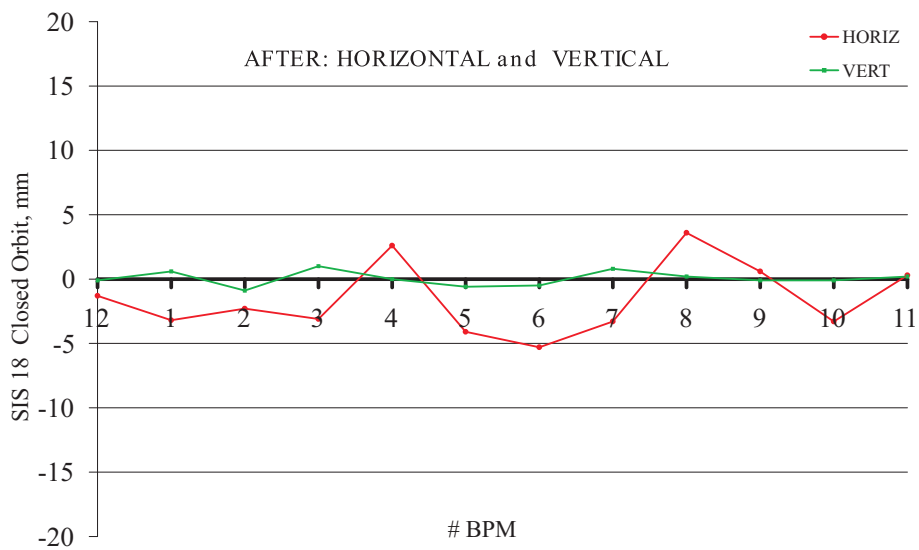


Figure 14: The horizontal and vertical CO at extraction energy after correction.

taken into account to be sure in the measured beam position displayed by the POSI or by the scope. The horizontal correction was performed not as accurate as the vertical one because of the lack of steerers (only 6 at injection and 8 at extraction) in this plane. It was also checked that the correction setting found provides a corrected CO which is not

sensitive to different extraction energies in the range of [100;1000] Mev/u.

We have checked the robustness of the correction by changing the tune from (4.29, 3.29) to (4.17, 3.35) and keeping the correction steerers unchanged. We found no relevant changes. We tried to understand these results by changing the tune in the MAD simulation in Figs. 7 and 8. In the vertical plane we did not find visible effect on the CO by changing the tune. In the horizontal plane the effect is larger, but still acceptable. This suggests that the dipolar errors in the SIS18 are not sensitive to the tune in the range explored.

Table 4: The steering angles for horizontal correction.

Period number	Name of steerer at injection	Value setting at injection	Name of steerer at extraction	Value setting at extraction
1	S01MU1A.1	-0.965	S01MU1A.2	-0.993
3	S03MU1A.1	0.335	S03MU1A.2	0.241
5	S05MU1A.1	1.036	S05MU1A.2	1.742
6	S06MU2A.1	1.190	S06MU2A.2	1.900
9	S09MU1A.1	-0.741	S09MU1A.2	0.000
12	S12MU1A.1	-0.387	S12MU1A.2	-0.387
10	—	—	S10MU1A.2	-0.990
11	—	—	S11MU1A.2	-0.217

6 Conclusion and Outlook

The CO measurements and ORM measurements were performed in several campaigns in SIS18. The horizontal and vertical SIS18 CO was corrected using the three-steerers local bump method. The local bump method has shown that all steerers appear to be well calibrated. The horizontal correction is not as perfect as the vertical, because of the lack of steerers. Tests performed with optimized multiturn injection have shown that after the CO is corrected the intensity of the beam increased at least by a factor of 2 as a result of an obtained larger machine acceptance.

It should be added that the present correction scheme does not represent the best optimization for SIS18. In fact maximum acceptance do not necessarily correspond to a flat CO. Only by using the modeling of SIS18 via the ORM and including all machine insertions, the optimization study will be completed.

Table 5: The steering angles for vertical correction.

Period number	Name of steerer at injection	Value setting at injection	Name of steerer at extraction	Value setting at extraction
1	S01KM2DV_1	0.163	S01KM2DV_2	-0.146
2	S02KM2DV_1	-0.496	S02KM2DV_2	-0.017
3	S03KM2DV_1	0.025	S03KM2DV_2	-0.135
4	S04KM2DV_1	-0.368	S04KM2DV_2	-0.023
5	S05KM2DV_1	-0.379	S05KM2DV_2	-0.529
6	S06KM2DV_1	0.375	S06KM2DV_2	0.284
7	S07KM2DV_1	-0.441	S07KM2DV_2	-0.241
8	S08KM2DV_1	-0.417	S08KM2DV_2	-0.065
9	S09KM2DV_1	-0.245	S09KM2DV_2	-0.184
10	S10KM2DV_1	-0.088	S10KM2DV_2	-0.039
11	S11KM2DV_1	-0.500	S11KM2DV_2	-1.000
12	S01KM2DV_1	-0.177	S01KM2DV_2	0.123

Further measurements are needed to assess the effect of CO correction on resonance excitation.

7 Acknowledgments

We would like to thank S.Y. Lee for his great help in applying the CO local bump method at GSI; I. Hofmann for his advice and suggestions; the diagnostics and BEL groups for technical support in particular P. Forck, J. Schölles, G. Fröhlich; SIS18 operator team in particular U. Scheeler, C. Wetzler, W. Kaufmann; P. Spiller for assistance in experiments and machine operations.

References

- [1] G. Franchetti, T. Giacomini, M. Kirk, A. Parfenova, "Resonance Induced Beam Loss in SIS18", GSI-Acc-Note-2005-12-001, GSI, Darmstadt, Germany, pp.11, <https://www.gsi.de/onTEAM/beschleuniger/notizen/public/GSI-Acc-Note-2005-12-001.pdf>

- [2] P. Kowina, W. Kaufmann, J. Schölles and M. Schwickert, "Optimization of "Shoe-box type" beam positions monitors using the finite element method", in Proc. DIPAC-2005, p. 114, Lyon, France, http://www-bd.gsi.de/conf/dipac05/dipac05_kowina.pdf.
- [3] X. Huang, S.Y. Lee, Eric Prebys, Chuck Ankenbrandt, "Fitting the Fully Coupled ORM for the Fermilab Booster", <http://lss.fnal.gov/archive/2005/conf/fermilab-conf-05-115-ad.pdf>.
- [4] S.Y. Lee "Accelerator Physics" Second Edition, World Scientific Publishing Co. Pte. Ltd. 2004, pp.124.
- [5] <http://bel.gsi.de/mk/operating/posi/posi.html>
- [6] Private G. Fröhlich, communication.